Supporting information

New prodrugs and analogs of the phenazine 5,10-dioxide natural products iodinin and myxin promote selective cytotoxicity towards human acute myeloid leukemia cells

Elvar Örn Viktorsson[a,b], Reidun Aesoy[c], Sindre Støa[a], Viola Lekve[c], Stein Ove Døskeland[d], Lars Herfindal[c] and Pål Rongved[a]

[a] *School of Pharmacy, Department of Pharmaceutical Chemistry, University of Oslo, PO Box 1068 Blindern, N0316 Oslo, Norway.*
[b] *School of Health Sciences, Faculty of Pharmaceutical Sciences, University of Iceland, Hofsvallagata 53, IS-107 Reykjavik, Iceland*
[c] *Centre for Pharmacy, Department of Clinical Science, University of Bergen, Jonas Lies vei 87, N-5021 Bergen, Norway*
[d] *Department of Biomedicine, University of Bergen, Jonas Lies vei 91, N-5021 Bergen, Norway*

**Corresponding author*: pal.rongved@farmasi.uio.no

KPLS-model of activity of iodinin-analogs towards MOLM-13 and NRK cells, and for identification of hypoxia-relevant moieties.

1: Generation of a KPLS model

All analogs listed in Table 1 in the main article as well as some from a previous publication on iodinin analogs [1] were imported into Canvas (ver. 4.1.013, MMshare Version 4.7.013, Schrödinger Software Modules, LLC, NY, 2019) [2] from .mol files.
The activity towards cell lines (EC50 from Table 1 or from [1]) were presented as *-log(EC50)* or *p(activity)* to linearize data and to ensure that the data were presented with higher value corresponding to high activity. The physico-chemical properties of all compounds were generated in Canvas using Task>properties>calculate. The properties were: Molecular weight (MW), hydrogen bond acceptor number (HBA), hydrogen bond donors (HBD), number of rotatable bonds (RB), heavy atom count, chiral center count, ring count, electronegativity state (Estate), molar refractivity (MR), partition coefficient (AlogP), polar surface area (PSA). See Table S1 at the end of this document for a list of all compounds and experimental and calculated properties. Next, dendritic fingerprint of each compound was created and kerne-based partial least square (KPLS) model was built using activity towards a given cell lines or hypoxia/normoxia as Y variable, and the calculated binary fingerprint as the X variable. Further settings were: Maximum number of KPLS factors = 3, 70% training set and 30% test set, where the same seed was used for all activities to ensure that the same compounds were used as training and test compounds at the different conditions. Images were exported from the visualize model function in the KPLS window. Atoms contributing to high activity is labelled green, whereas atoms contributing to low activity is labelled red.

2: Regression analyses and correlation fits for the KPLS models

2.1 Results from Molm-13 normoxiadata:

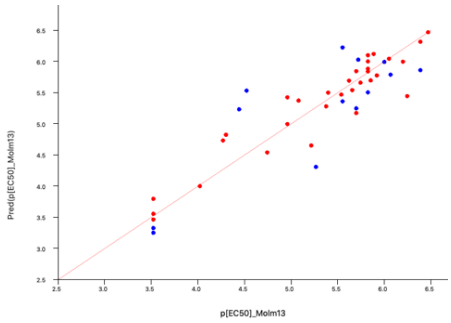

Rˆ2 after 2 KPLS factors was 0.8435 for the training set, and the Qˆ2 (correlation fit) for the test set was 0.7092, which was consider satisfactory. The scatter plot shows nice correlation. This suggests that the model can predict the activity of a compound based on its structure with acceptable accuracy.

2.2 Results from NRK normoxia data

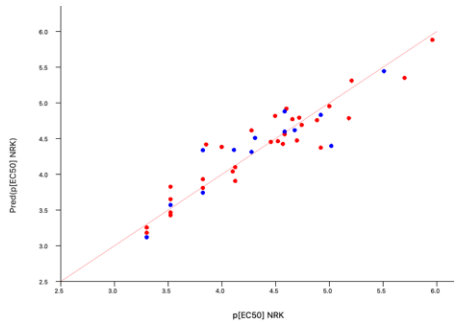

Rˆ2 after 2 KPLS factors was 0.8139, and after 3 factors, it was 0.8755. The Qˆ2 was 0.8542 after 2 factors, and 0.8135 after 3 factors. The scatter plot after 3 factors confirms the good correlation, and this model can be used to predict structures based on activity.

2.3 Results from Molm-13 hypoxia data

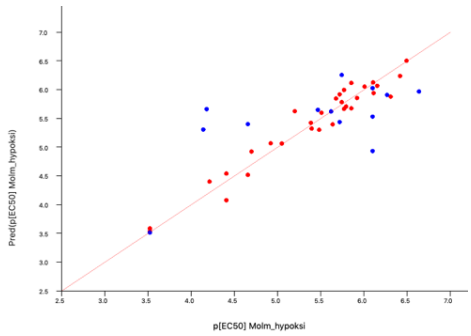

Rˆ2 after 3 KPLS factors was 0.9431, and the Qˆ2 for the test set was 0.3966. There are obviously a few compounds or chemical moieties which are difficult to predict with respect to activity under hypoxic conditions. The scatter plot shows that the activity of structure **12** and **13** are heavily overestimated, whereas the activity of structure 3 (iodinin) is underestimated by a value of around one (p[EC50] value, means a factor of ten in concentration). For structure **12** and **13**, the problem can be that both have very low permeability (see Table 1 in the main article), perhaps due to chelation with cations in the medium. Such events are not predicted by the model. Furthermore, hypoxia experiments are very dependent on stable conditions, and small variations in oxygen saturation in the incubators would have larger impact on these data compared to those obtained under normoxic conditions.

2.4 Results from NRK hypoxia data

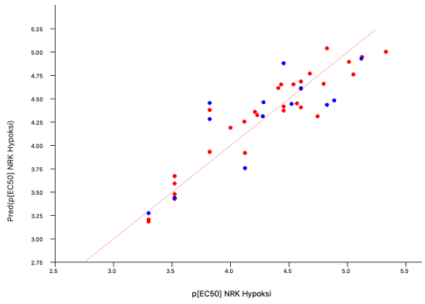

Rˆ2 after 3 KPLS factors was 0.8738, and the Qˆ2 for the test set was 0.6267. This is a bit lower than for NRK normoxia data, but still decent correlation, and we conclude that this model can be used to predict activity under hypoxic conditions. There were two outliers, where the predicted activity was overestimated. As with Molm-13 data, these were structure **12** and **13**.

3: Comparison between predictions for activity, MOLM-13 vs. NRK.

Here, we compare the predicted contribution of each parts of the molecules with respect to activity towards MOLM-13 and NRK. We focus on differences between activity towards Molm-13 and NRK cells, and between MOLM-13 cells cultured under normoxic and hypoxic conditions.

3.1 Visualization of KPLS model on MOLM-13 cells

We noticed first that the oxygens, but not the nitrogens, of the N-oxides were considered neutral. The charged nitrogens are predicted with high activity. One explanation to why the N-oxides fail to be predicted with high activity contrary to our findings with myxin-analogs lacking N-oxides [1], can be that such moieties are considered weak spots for in silico modelling [3]. Interestingly, the oxygen of the N-oxides was considered important for Molm-13 activity when there was an -OMe substituent in position 6 instead of -OH (as in iodinin). Further, structures **1-12** and **1-14** (myxin, but lacking one or both oxygens on the nitrogens) was correctly predicted as having very low activity, and here the non-oxygenated nitrogen was associated with reduced activity. The -OH groups in position 1 and 6 are associated with high activity but not to the same extent as the nitrogens (positions 5 and 10 of the scaffold).

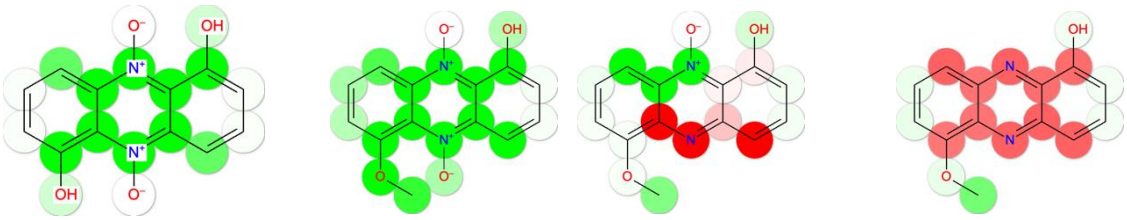

Structure **3** (iodinin) and **4** (myxin) and the de-oxygenated forms of myxin (**1-12** and **1-14**).

Substituents which stood out as having negative impact on activity towards MOLM-13 cells were the pivalate esters on compound **11**, the valerate esters of compound **12** and the ethyl carbonate side chain on compound **13**. The methyl groups in positions 7 and 8 (compounds **44**, **48** and **52**) resulted in negative impact on MOLM-13 activity as well. All two-ring compounds were correctly predicted as having poor activity. According to the model, the linker was also important for activity, and when O-*tert*butyl acetate side chains (2-(tert-butoxy)-2-oxoethoxy) was attached to the phenols (structure **1-18**) instead of the pivalic esters (structure **11**) they were associated with high activity. This means that not only the end-substituent, but also the linker is important for activity. This can be explained with the concept of prodrug, where the stability of the linker in medium and in the cytoplasm can be a determinant for activity.

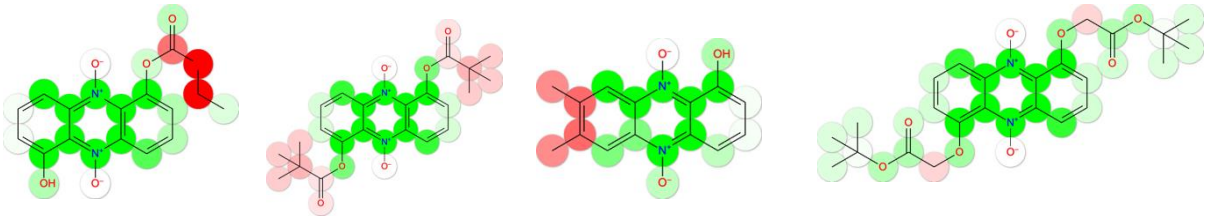

Structure **13**, **11**, **44**, and **1-18**. Notice the difference between the *tert*-butyl based substituents in structure **11** and **1-18**, suggesting that the linker is a determining factor for activity for these structures.

In general, a short linker consisting of carbamate bond was associated with high activity even when added different substituents like the pyrrolidine ring in structure **19**, the *N,N*-dimethyl of **structure 20** or the piperazine of structure **18**. Note that in all these cases, the linker ends with a nitrogen (a carbamate), whereas in structure **13** (a carbonate), the linker ends with an oxygen, which is associated with low activity.

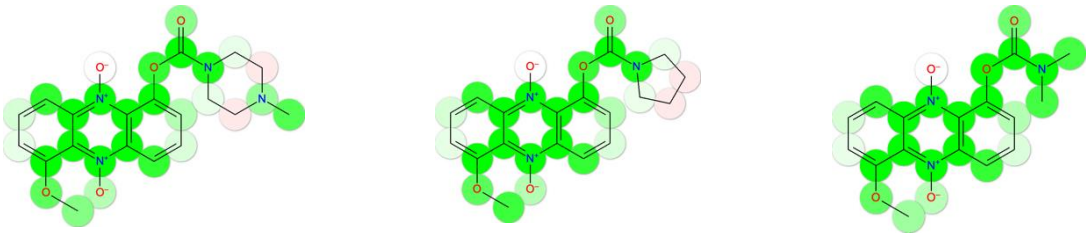

Structures **18**, **19**, and **20**. Note that the nitrogen in the carbamate functional group is associated with high activity, whereas in structure 13, the nitrogen is replaced by an oxygen forming a carbonate functionality and results in low activity.

3.2 Visualization of KPLS model on NRK cells

In general, the effect of the different analogs on MOLM-13 cells was reflected in their activity towards NRK, except that most analogs were much less potent towards NRK cells. A large difference in predictions was therefore not expected. However, it was predicted that the two -OH groups in position 1 and 6 on iodinin (**3**) was linked to low activity. This was also the case for all structures with one or more phenols (-OH). As such, it appears that mono-substituted analogues should have higher selectivity towards Molm-13 cells than di-substituted analogues.

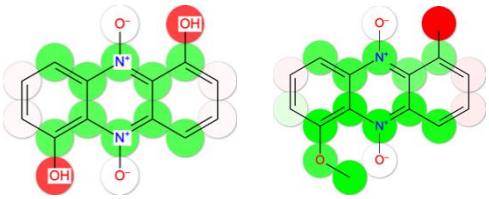

Structure 3 (iodinin) and 4 (myxin). Note that the phenol -OH in position 1 and 6 are associated with low activity, in contrast to the model on MOLM-13.

Besides this, there were several molecular elements which were common for high activity in MOLM-13 and NRK cells, such as the pivalate esters in structure **11** being a predictor for low activity whereas the carbamate nitrogen atom in structures **16**, **17**, **15**, **20**, and **18** was associated with high activity. The fourth ring in the tetracyclic structure **53** was associated with high activity in NRK-cells but was neutral in the model for MOLM-13 cells. This suggests that the introduction of a fourth ring shifts the activity of the compounds from being AML selective to a more general cytotoxic activity which does not discriminate between cancerous and non-cancerous cells.

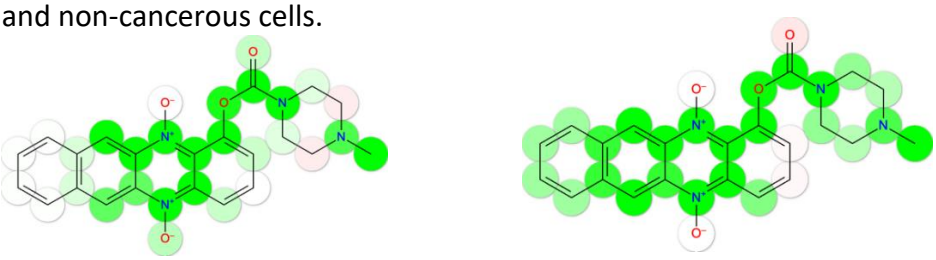

The predicted atomic contribution of structure **53** towards AML activity (left) or NRK activity (right). Notice that while the terminal aromatic ring is predicted to be neutral towards AML cells, it is predicted to contribute to high activity in NRK-cells.

3.3 Comparison of the KPLS models on MOLM-13 activity cells obtained under normoxic and hypoxic conditions

Here, we can see a clear difference in the two models for tirapazamine (structure **10**). Whereas the nitrogens are clearly associated with poor activity in normoxic conditions, they are associated with high activity in hypoxic conditions. Although this could give indications on how to create hypoxia-dependent analogues, this is only one example, and more analogs of tirapazamine should be part of a KPLS-model before we can conclude on the importance of the nitrogens in the *N*-oxide-containing ring.

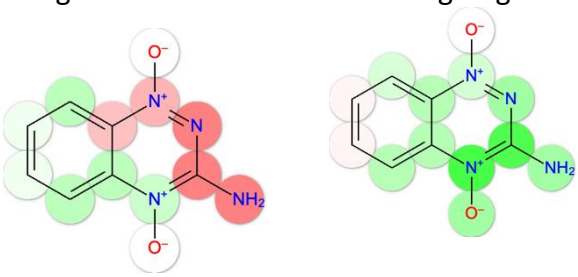

The atomic contribution for low and high activity of structure 10 (tirapazamine) in normoxic (left) and hypoxic (right) conditions.

No large differences were found in structure 3 (iodinin), or structure 4 (myxin). Some of the linkers, such as the ethyl- and *tert*butyl acetate side chains in structures **24** and **25** were connected to poor activity to a higher degree in hypoxia, which could be related to the activation of the prodrug being slower in hypoxic conditions.

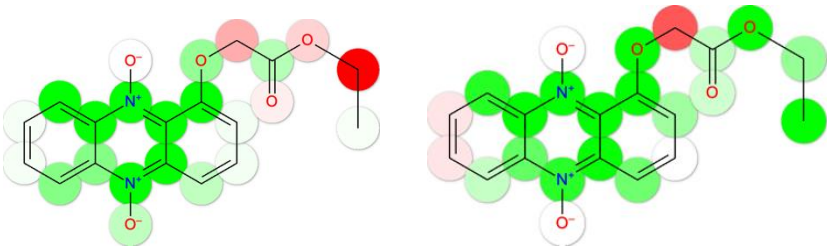

Predicted atomic contribution for activity for structures **24** under normoxic (left) and hypoxic (right) conditions. Note that the -CH_2- in the linker is predicted to be associated with low activity.

Another difference was the influence of methyl groups in positions 7 and 8 on the phenazine scaffold, where the methyl groups were linked to high activity in hypoxic conditions, but not in normoxic conditions. This was evident in structures **44** (illustrated), **48**, and **52**.

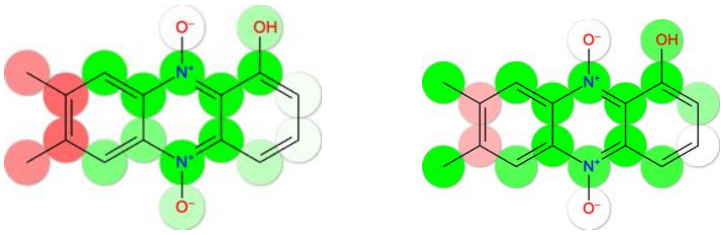

Structure **44**, with predicted atomic contribution to activity in normoxic (left) and hypoxic (right) conditions. Note the Me-substituents in position 7 and 8.

Table 1: Structures and their cytotoxicity and molecular properties used to create dendritic fingerprinting. Structures 1-11 to 1-20 corresponds to a previously published study (reference no.: 2, Viktorsson et al. 2017)

Structure	Name	Permeability (Log)	p[EC50] MOLM-13	p[EC50] NRK	p[EC50] Molm hypoksi	p[EC50] NRK Hypoksi	MW	HBA	HBD	RB	Heavy Atom Count	Chiral Center Count	Chiral Center Count All Possible	Ring Count	Estate	MR	AlogP	PSA
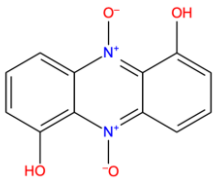	Structure_3	-5,64	5,699	4,125	6,102	4,125	244,2029	2	2	5,699	5,699	0	0	3	56,002	56,169	-2,8556	94,34
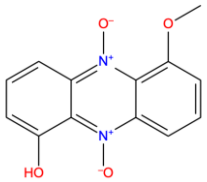	Structure_4	-4,94	5,854	4,114	6,114	4,119	258,2295	2	1	5,854	5,854	0	0	3	55,502	60,9381	-2,6046	83,34
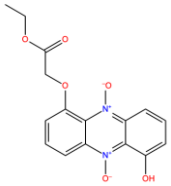	Structure_7	-4,84	6,244	4,921	6,31	4,744	330,2922	4	1	6,244	6,244	0	0	3	70,669	76,5398	-2,5487	109,64

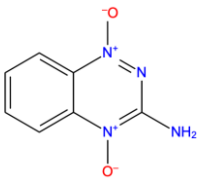	Structure_10	-5,79	4,022	3,824	4,658	4,456	178,1481	1	-5,79	-5,79	4,022	0	0	2	42,001	42,7503	-2,3606	92,79
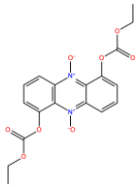	Structure_14	-4,75	5,215	4,456	5,398	4,456	388,3282	6	0	5,215	5,215	0	0	3	82,336	87,7888	-0,8014	124,94
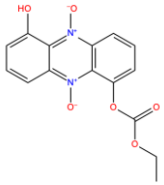	Structure_13	-7,32	4,301	3,824	4,181	3,824	316,2656	4	1	4,301	4,301	0	0	3	69,169	71,9789	-1,8285	109,64
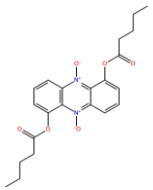	Structure_12	-7,74	4,444	3,824	4,658	3,824	412,4358	4	0	4,444	4,444	0	0	3	81,336	102,7034	0,3732	106,48

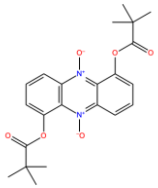	Structure_11	-6,06	4,959	3,824	5,051	3,824	412,4358	4	0	4,959	4,959	0	0	3	82,836	102,4504	0,3072	106,48
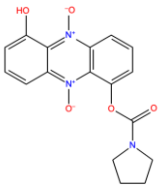	Structure_16	-4,74	6,066	5,018	6,102	4,824	341,3181	3	1	6,066	6,066	0	0	4	70,169	82,0156	-1,6332	103,65
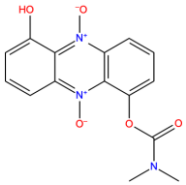	Structure_17	-5,06	6,051	4,31	6,155	4,208	315,2808	3	1	6,051	6,051	0	0	3	68,169	74,4754	-2,0942	103,65
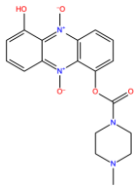	Structure_15	-5,96	5,824	4,276	5,854	4,229	370,3593	3	1	5,824	5,824	0	0	4	74,169	90,5255	-2,1369	106,89

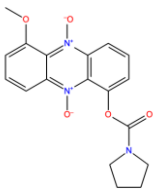	Structure_19	-5,1	5,699	4,495	5,745	4,456	355,3447	3	0	5,699	5,699	0	0	4	69,669	86,7847	-1,3822	92,65
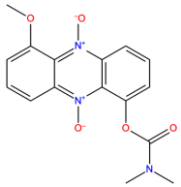	Structure_20	-5,1	5,721	4,658	5,77	4,538	329,3074	3	0	5,721	5,721	0	0	3	67,669	79,2445	-1,8432	92,65
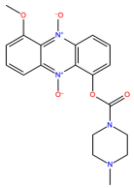	Structure_18	-5,74	6	4,585	6,009	4,409	384,3859	3	0	6	6	0	0	4	73,669	95,2946	-1,8859	95,89
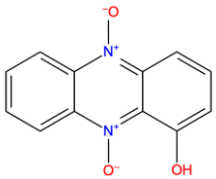	Structure_21	-4,74	4,959	4,102	4,921	3,824	228,2035	1	1	4,959	4,959	0	0	3	50,335	54,4749	-2,5882	74,11

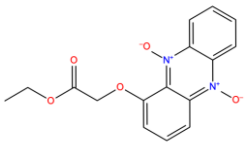	Structure_24	-4,93	5,824	4,585	5,77	4,602	314,2928	3	0	5,824	5,824	0	0	3	65,002	74,8457	-2,2813	89,41
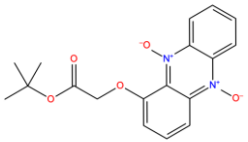	Structure_25	-4,76	5,657	4,585	5,721	4,602	342,3459	3	0	5,657	5,657	0	0	3	68,752	83,9015	-1,6988	89,41
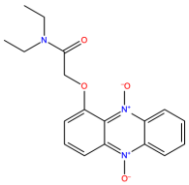	Structure_26	-5,2	5,921	4,886	5,854	4,796	341,3612	2	0	5,921	5,921	0	0	3	67,002	86,4402	-2,3739	83,42
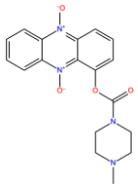	Structure_27	-4,85	5,824	4,602	5,721	4,432	354,3599	2	0	5,824	5,824	0	0	4	68,502	88,8314	-1,8695	86,66

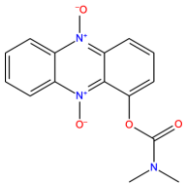	Structure_28	-4,95	5,886	4,721	5,678	4,602	299,2814	2	0	5,886	5,886	0	0	3	62,502	72,7813	-1,8268	83,42
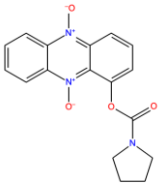	Structure29	-4,91	5,824	4,744	5,921	4,678	325,3187	2	0	5,824	5,824	0	0	4	64,502	80,3215	-1,3658	83,42
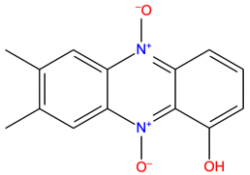	Structure_44	-5,45	5,553	4,125	5,638	4,125	256,2567	1	1	5,553	5,553	0	0	3	53,669	64,5573	-1,6158	74,11
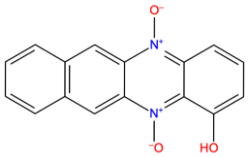	Structure_45	-7,23	4,523	4	4,699	4	278,2622	1	1	4,523	4,523	0	0	4	57,669	70,9251	-1,6798	74,11

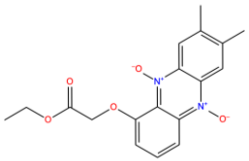	Structure_48	-4,93	5,081	3,854	5,201	3,824	342,3459	3	0	5,081	5,081	0	0	3	68,336	84,9281	-1,3089	89,41
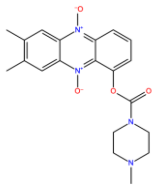	Structure_52	-4,97	6,201	4,921	6,268	4,886	382,4131	2	0	6,201	6,201	0	0	4	71,836	98,9138	-0,8971	86,66
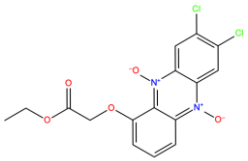	Structure_50	-5,16	6,387	5,509	6,42	5,328	383,1829	3	0	6,387	6,387	0	0	3	72,558	84,4553	-0,9525	89,41
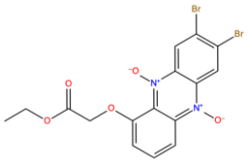	Structure_51	-5,24	5,62	5	5,796	5,013	472,0849	3	0	5,62	5,62	0	0	3	69,836	90,0913	-0,7845	89,41

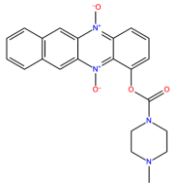	Structure_53	-5,26	5,553	5,699	5,745	5,125	404,4186	2	0	5,553	5,553	0	0	5	75,836	105,2816	-0,9611	86,66
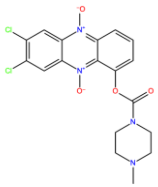	Structure_54	-4,97	6,469	5,959	6,495	4,824	423,25	2	0	6,469	6,469	0	0	4	76,058	98,441	-0,5407	86,66
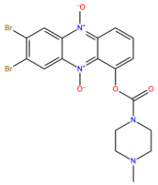	Structure_55	-4,88	6,387	5,208	6,638	5,119	512,152	2	0	6,387	6,387	0	0	4	73,336	104,077	-0,3727	86,66
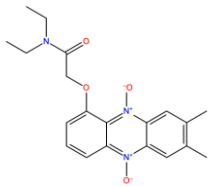	Structure_56	-5,18	5,745	4,678	5,469	4,284	369,4143	2	0	5,745	5,745	0	0	3	70,336	96,5226	-1,4015	83,42

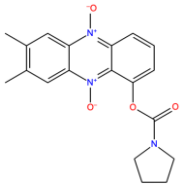	Structure_57	-4,85	5,823	5,181	6,108	5,051	353,3719	2	0	5,823	5,823	0	0	4	67,836	90,4039	-0,3934	83,42
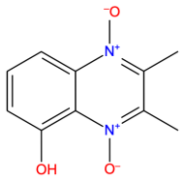	Structure_60	-4,35	3,523	3,301	3,523	3,301	206,198	1	1	3,523	3,523	0	0	2	46,335	48,5679	-3,7884	74,11
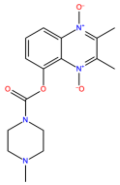	Structure_61	-4,48	3,523	3,301	3,523	3,301	332,3544	2	0	3,523	3,523	0	0	3	64,502	82,9244	-3,0697	86,66
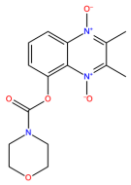	Structure_62	-4,65	3,523	3,301	3,523	3,301	319,3126	3	0	3,523	3,523	0	0	3	64,002	75,9488	-3,3393	92,65

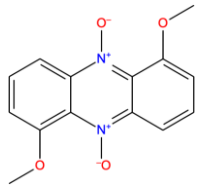	Structure_1_11	-5,1	5,398	4,699	5,509	4,602	272,2561	2	-5,1	-5,1	5,398	0	0	3	55,002	65,7072	-2,3536	72,34
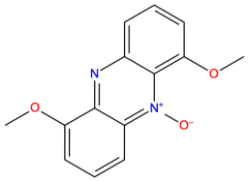	Structure_1_13	-5,1	5,267	3,522	5,387	3,523	256,2567	3	-5,1	-5,1	5,268	0	0	3	47,002	65,8951	0,3366	58,29
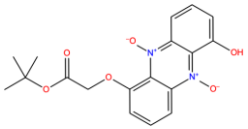	Structure_1_17	-5,04	5,538	4,276	5,62	4,276	358,3453	4	-5,04	-5,04	5,538	0	0	3	74,419	85,5956	-1,9662	109,64
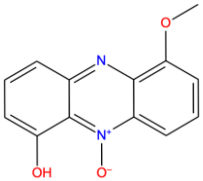	Structure_1_12	-5,09	3,523	3,523	4,143	3,523	242,2301	3	-5,09	-5,09	3,523	0	0	3	47,502	61,126	0,0856	69,29

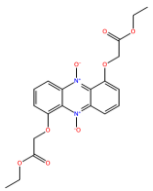	Structure_1_16	-5,17	5,699	4,523	6,102	4,523	416,3814	6	-5,17	-5,17	5,699	0	0	3	85,336	96,9106	-2,2418	124,94
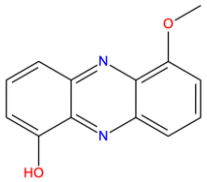	Structure_1_14	-5,08	3,523	3,523	4,409	3,523	226,2307	4	-5,08	-5,08	3,523	0	0	3	39,502	61,3139	2,7758	55,24
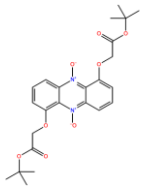	Structure_1_18	-5,2	5,377	4,569	5,482	4,569	472,4877	6	-5,5	-5,5	5,377	0	0	3	92,836	115,0222	-1,0768	124,94
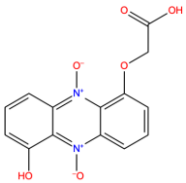	Structure_1_19	-7,16	4,268	3,523	4,215	3,523	302,239	2	-7,16	-7,16	4,268	0	0	3	70,669	67,0227	-3,1485	120,64

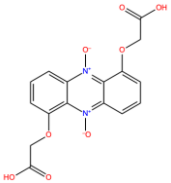	Structure_1_20	-7,2	4,745	3,523	4,409	3,523	360,2751	2	-7,2	-7,2	4,745	0	0	3	85,336	77,8764	-3,4414	146,94

References

1. Viktorsson, E.O., et al., *Total synthesis and antileukemic evaluations of the phenazine 5,10-dioxide natural products iodinin, myxin and their derivatives.* Bioorg Med Chem, 2017. **25**(7): p. 2285-2293.
2. Duan, J., et al., *Analysis and comparison of 2D fingerprints: insights into database screening performance using eight fingerprint methods.* J Mol Graph Model, 2010. **29**(2): p. 157-70.
3. Eros, D., et al., *Reliability of logP predictions based on calculated molecular descriptors: a critical review.* Curr Med Chem, 2002. **9**(20): p. 1819-29.